

Short Communication

## Enhancing the Magnetic Properties and Corrosion Resistance of Sintered NdFeB Magnets by Diffusion Process

Yong Gu<sup>1, \*</sup>, Sihao Hua<sup>2</sup>, Minxiang Pan<sup>2</sup>, Xiani Huang<sup>2</sup>

<sup>1</sup> Qianjiang College, Hangzhou Normal University, Hangzhou, 310036, P. R. China

<sup>2</sup> Zhejiang Fangyuan Test Group Co., LTD, Hangzhou, 310018, China

\*E-mail: [guyonghz@126.com](mailto:guyonghz@126.com) (Yong Gu)

Received: 18 December 2019 / Accepted: 14 January 2020 / Published: 10 March 2020

Low melting point Ce-Al-Cu alloy was employed as the grain boundary diffusion source to prepare the NdFeB sintered magnets. Compared to the original Nd-Fe-B magnet, the coercivity  $H_{cj}$  can get 36.7 % increments for the Ce-Al-Cu diffused magnet. Meanwhile, the microstructure of the diffused magnet has been refined with the grain size of 10~20  $\mu\text{m}$  and the corrosion potential  $E_{\text{corr}}$  is increased to -0.68 V. Further investigation of mass loss of magnets in hot/humid atmosphere demonstrates that the addition of low melting point alloys can improve the corrosion resistance of NdFeB sintered magnets.

**Keywords:** Corrosion; NdFeB; Magnetic properties; Diffusion

### 1. INTRODUCTION

With the expanding application field and increasing demand of rare earth permanent magnets, a large number of key rare earth elements (Pr, Nd, Dy, Tb, etc.) are consumed excessively, while the rich and abundant rare earth elements (La, Ce, Y, etc.) are overstocked [1]. High abundance rare earth permanent magnets can not only reduce production costs, but also achieve rarity. Considering the strategic safety of national rare earth resources, the production cost of raw materials and the sustainable development of rare earth industry, the comprehensive and balanced utilization of land resources has become one of the hotspots in the research and development of rare earth permanent magnets with high performance-price ratio and high abundance. In recent years, many researchers have carried out extensive research on high-value balanced utilization of high-abundance rare earth permanent magnets [2-6].

In addition, the grain boundary diffusion (GBD) method has attracted wide attention to prepare the low rare-earth and high magnetic performance of the Nd-Fe-B magnets [7-11]. The GBD method firstly needs to attach a layer of rare earth alloy or compound on the surface of the magnet. After heat treatment, rare earth elements gradually permeate from the surface to the interior of the magnet along

the grain boundary, and diffuse from the grain boundary phase to the main phase. H. Sepehri-Amin et al. [12] found that after diffusion through grain boundaries, rare earth shells formed between the main phase grains and the grain boundaries, which promoted the magnetic hardening of the main phase grains. Meanwhile, Zhang et al. [13] demonstrated that Cu and Zr co-addition can result in relevant improvement in the magnetic properties, electrochemical stability and corrosion resistance. However, the magnetic properties of the NdFeB magnets are still not impressive, especially for the coercivity ( $H_{cj}$ ) remains not significantly improved and the preparation process is relatively complex.

In this paper, in order to further enhance the magnetic properties of NdFeB magnets, the effects of the Ce-Al-Cu diffused on the magnetic properties, microstructure, and corrosion resistance of the NdFeB magnet are systematically investigated.

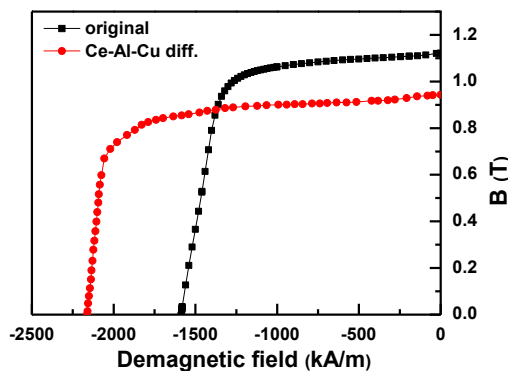
## 2. EXPERIMENTAL PART

The sintered NdFeB alloy with the composition of  $\text{Nd}_{14.63}\text{Pr}_{4.52}\text{Fe}_{72.96}\text{Cu}_{0.16}\text{Al}_{1.47}\text{Nb}_{0.21}\text{B}_{6.03}$  (at. %) was used as the original magnet with the size of  $\Phi 10 \times 5$  mm, which was prepared by the traditional powder metallurgical technology and then by polished the surface of the magnet, remove the surface lines, oil impurities, etc., and use the polished and cleaned magnet as the diffusion matrix. The low melting point Ce-Al-Cu alloy with the composition of  $\text{Ce}_{65}\text{Al}_{15}\text{Cu}_{20}$  was prepared by arc melting for four times to ensure homogeneity under high purity Ar atmosphere and subject to by melt-spun method onto the Cu crucible in an argon atmosphere with a wheel speed of 25 m/s. As-quenched Ce-Al-Cu ribbons were milled for 3 hours as the diffusion sources by the high-energy ball milling (HEBM, Spex-8000M). The height of the diffusion sources (Ce-Al-Cu powders) on the surface of the NdFeB magnet is 1.5 mm. The diffusion treatments were performed at 600 ~ 850 °C for 3 ~ 5 h in the vacuum of lower than  $5 \times 10^{-4}$  Pa.

The phase constitution and microstructure of the magnets were analyzed by the Rigaku D/max 2500 X-ray diffraction (XRD) with a Cu  $K\alpha$  radiation (The wavelength of X-ray is  $\lambda = 1.5406$  Å, the scanning angle range is  $20^\circ \sim 100^\circ$ , the scanning step length is  $0.02^\circ$ , and the scanning speed is  $1^\circ/\text{min}$ ) and SEM (Hitachi-TM3000). The magnetic properties of the magnets were measured by the Pulsed Field Magnetometer (PFM) with the maximum magnetic field of 7.5 T. Polarization curves in 2.5 wt.% NaCl aqueous solution were determined with a PARSTAT 2273 advance electrochemical system. Accelerated corrosion test was performed by placing magnets in 120°C, 2 bar and 100% relative humid atmosphere for 24, 48, 72 and 96 h, respectively.

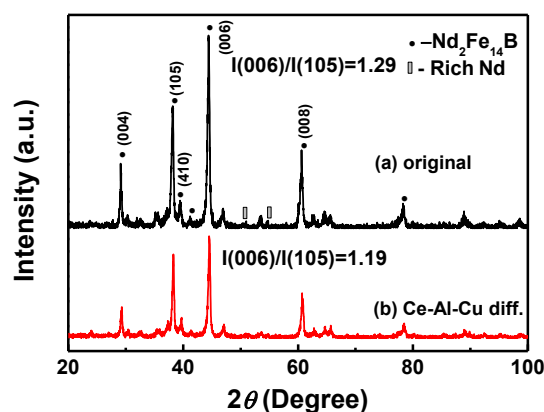
## 3. RESULTS AND DISCUSSION

Fig. 1 shows the demagnetization curves of the original magnet and Ce-Al-Cu diffused magnet. According to the magnetic properties results of Fig.1, the significant coercivity enhancement has been obtained for the Ce-Al-Cu diffused magnet. The coercivity  $H_{cj}$  is increased from 1582 kA/m to 2163 kA/m for the original magnet and Ce-Al-Cu diffused magnet, respectively. Compared to the original NdFeB magnet, the coercivity  $H_{cj}$  can get 36.7 % increments for the Ce-Al-Cu diffused magnet. However, the remanence  $B_r$  decreases from 1.12 T to 0.95 T as the reason of increasing volume fraction of non-magnetic phases in grain boundaries for the Ce-Al-Cu diffused and the Ce element enters into the main phase  $\text{Nd}_2\text{Fe}_{14}\text{B}$  phase [14,15].



**Figure 1.** Demagnetization curves of the original magnet and Ce-Al-Cu diffused magnet.

In addition, by the diffusion of Ce-Al-Cu into the NdFeB magnet, the maximum energy product  $(BH)_{\max}$  is decreased from  $239 \text{ kJ/m}^3$  to  $221 \text{ kJ/m}^3$  due to the low remanence  $B_r$  in the demagnetization curve.



**Figure 2.** XRD patterns of the original magnet (a) and Ce-Al-Cu diffused magnet (b).

Fig. 2 shows the XRD patterns of the original NdFeB magnet and with Ce-Al-Cu diffused NdFeB magnet. It can be seen that the diffraction peaks of two samples are from the  $\text{Nd}_2\text{Fe}_{14}\text{B}$  ( $P42/mnm$ ) hard magnetic phase and a small amount of the Nd-rich phase. Moreover, the intensities of (004), (006), (008) planes are much higher than that of (410) plane in  $\text{Nd}_2\text{Fe}_{14}\text{B}$  standard powder. This indicates that a strong (00L) orientation characteristic has been obtained for the two studied samples. To illustrate the degree of (00L) orientation characteristic in the magnets, the value of  $I(006)/I(105)$  is calculated in each sample shown in Fig. 2. The results showed that the value of  $I(006)/I(105)$  for the original magnet is 1.29, which is higher than the Ce-Al-Cu diffused magnet (1.19). It indicates that a low value of  $I(006)/I(105)$  for the diffused magnet results in lower remanence  $B_r$  and the maximum energy product  $(BH)_{\max}$ , indicating that the intensity of the orientation is decreased with Ce-Al-Cu diffusion, which is mainly due to the Ce element entering into the main phase  $\text{Nd}_2\text{Fe}_{14}\text{B}$  phase and reducing the anisotropy of the magnetocrystalline, which is consistent with the results for NdFeB magnets by PrGa-doped [16].

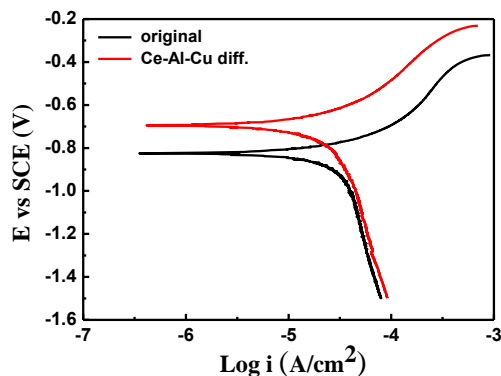


**Figure 3.** Polarization curves of the original magnet and Ce-Al-Cu diffused magnet in 2.5 wt.% NaCl solution.

To elucidate the contribution of low melting point Ce-Al-Cu alloy to the corrosion resistance of NdFeB magnets, the corrosive medium 2.5 wt.% NaCl solution is used for evaluating the corrosion inhibition from the magnets. Fig. 3 shows the polarization curves of the original magnet and Ce-Al-Cu diffused magnet at room temperature. In polarization curve analysis, the corrosion potential  $E_{corr}$  is usually used to characterize the degree of difficulty of corrosion in solution environment. The higher the corrosion potential, the more difficult it is to corrode. The corresponding results of the corrosion potential  $E_{corr}$  and corrosion current density  $i_{corr}$  obtain by the Tafel extrapolation method [17] is listed in Table 1. Compared to the original NdFeB magnet, the corrosion potential  $E_{corr}$  is increased from -0.82 V to -0.68 V for the Ce-Al-Cu diffused magnet. Besides, the corrosion current density  $i_{corr}$  is also decreased from 92.45  $\mu\text{A}/\text{cm}^2$  to 78.15  $\mu\text{A}/\text{cm}^2$ . It indicates that corrosion potential of the grain boundary phase can be significantly increased by adding low melting point Ce-Al-Cu alloy at grain boundary, which reduces the potential difference between the main phase and grain boundary [18], and improves the corrosion resistance of diffused NdFeB magnet.

**Table 1.** The corrosion potential  $E_{corr}$  and corrosion current density  $i_{corr}$  of the original magnet and Ce-Al-Cu diffused magnet tested in 2.5 wt.% NaCl aqueous solutions.

Alloy	$E_{corr}(\text{V})$	$i_{corr}(\mu\text{A}/\text{cm}^2)$
Original	-0.82	92.45
Ce-Al-Cu	-0.68	78.15

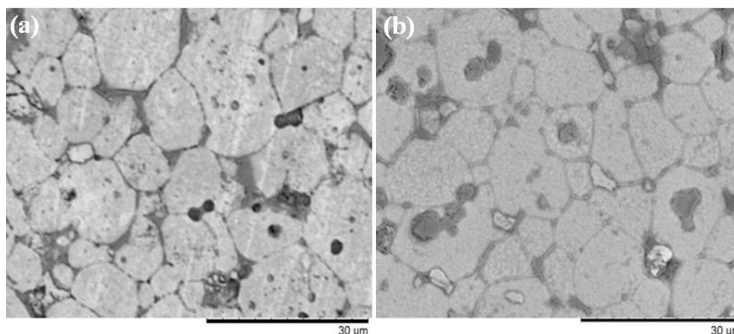


**Figure 4.** SEM images for the original magnet (a) and Ce-Al-Cu diffused magnet (b) after corrosion.

Fig. 4 displays the SEM images for the original magnet and Ce-Al-Cu diffused magnet after corrosion. As shown in Fig. 4 (a) for the original NdFeB magnet, it can be seen that there are some black holes in the permanent magnet, which may be due to the poor fluidity of liquid phase and insufficient thermal driving energy to make the small grains grow. The black holes disappear in the Ce-Al-Cu diffused magnet (Fig. 4 (b)). Meanwhile, compared to the original magnet, the grain size in the Ce-Al-Cu diffused magnet has been refined, where the average grain size of the original magnet and the diffused magnet is determined to be 15~25  $\mu\text{m}$  and 10~20  $\mu\text{m}$ , respectively. Furthermore, a small amount of flocculent oxide exists on the surface of the Ce-Al-Cu diffused magnet after corrosion, which is mainly due to the oxidation corrosion of Nd-rich phase at grain boundary and hydrogen absorption and pulverization caused by acid corrosion solution. Furthermore, the Nd-rich phase at grain boundary for the Ce-Al-Cu diffused magnet has good corrosion resistance, which is consistent with previous results of polarization curves.

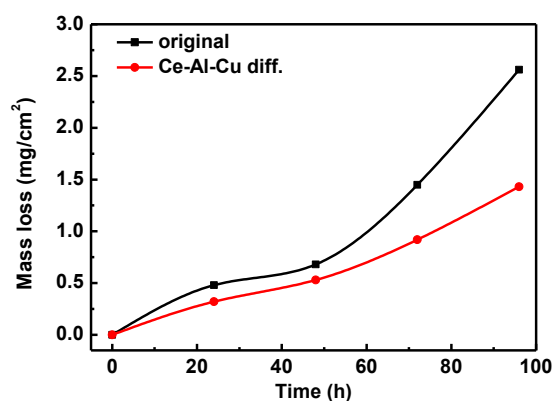


**Figure 5.** Mass loss of the original magnet and Ce-Al-Cu diffused magnet in hot/humid atmosphere for different times.

Corrosion resistance, as an important index of magnet service, is very important for the practical application of magnets. The corrosion resistance of Ce-Al-Cu diffused magnet in hot and humid environment will also be studied. Fig. 5 shows the mass loss of the original magnet and Ce-Al-Cu diffused magnet in hot/humid atmosphere for different times. Under the same test conditions, it can be seen that the mass loss of the original magnet and the Ce-Al-Cu diffused magnet before 60 hours is almost negligible, below 0.7  $\text{mg}/\text{cm}^2$ . As the test time increase to the 96 h, the mass loss for the original magnet and the Ce-Al-Cu diffused magnet reach to the 2.56  $\text{mg}/\text{cm}^2$  and 1.43  $\text{mg}/\text{cm}^2$ , respectively. The mass loss for the Ce-Al-Cu diffused magnet is obvious lower than the original NdFeB magnet. It means that the addition of low melting point Ce-Al-Cu alloys can improve the corrosion resistance of NdFeB sintered magnets in hot/humid atmosphere environment. Similar to the results for the NdFeB magnets by other low melting point intergranular addition [19,20].

#### 4. CONCLUSION

The corrosion resistance of NdFeB magnets can be enhanced with the low melting point Ce-Al-Cu alloy by the grain boundary diffusion method. The coercivity is increased from 1582 kA/m to 2163 kA/m for the original magnet and Ce-Al-Cu diffused magnet, respectively. Furthermore, compared to

the original NdFeB magnet, the corrosion current density  $i_{\text{corr}}$  is also decreased from  $92.45\mu\text{A}/\text{cm}^2$  to  $78.15\mu\text{A}/\text{cm}^2$ , indicates that corrosion potential of the grain boundary phase can be significantly increased. Further investigation of mass loss of magnets in hot/humid atmosphere demonstrates that the addition of low melting point alloys can improve the corrosion resistance of NdFeB sintered magnets.

## References

1. R.W. McCallum, L. Lewis, R. Skomski, M.J. Kramer, I.E. Anderson, *Annu. Rev. Mater. Res.*, 44 (2014) 451.
2. D. Li, Y. Bogatin, *J. Appl. Phys.*, 69 (1991) 5515.
3. T.W. Capehart, R.K. Mishra, G.P. Meisner, C.D. Fuerst, J.F. Herbst, *Appl. Phys. Lett.*, 63 (1993) 3642.
4. X.D. Fan, S. Guo, K. Chen, R.J. Chen, D. Lee, C.Y. You, A.R. Yan, *J. Magn. Magn. Mater.*, 419 (2016) 394.
5. J. Chaboy, A. Marcelli, J. García, H. Maruyama, L.M. García, K. Kobayashi, L. Bozukov, *J. Magn. Mater.*, 140-144 (1995) 1213.
6. A. Alam, M. Khan, R.W. McCallum, D.D. Johnson, *Appl. Phys. Lett.*, 102 (2013) 042402.
7. N. Watanabe, M. Itakura, M. Nishida, *J. Alloys Compd.*, 557 (2013) 1.
8. K.H. Bae, S.R. Lee, H.J. Kim, M.W. Lee, T.S. Jang, *J. Appl. Phys.*, 118 (2015) 297.
9. K. Hirota, H. Nakamura, T. Minowa, M. Honshima, *IEEE Trans. Magn.*, 42 (2006) 2909.
10. F. Xu, J. Wang, X. Dong, L. Zhang, J. Wu, *J. Alloy Compd.*, 509 (2011) 7909.
11. X. Liu, X. Wang, L. Liang, P. Zhang, J. Jin, Y. Zhang, T. Ma, M. Yan, *J. Magn. Magn. Mater.*, 370 (2014) 76.
12. H. Sepehri-Amin, T. Ohkubo, S. Nagashima, M. Yano, T. Shoji, A. Kato, T. Schrefl, K. Hono, *Acta Mater.*, 61 (2013) 6622.
13. M.X. Pan, P.Y. Zhang, Q. Wu, H.L. Ge, *Int. J. Electrochem. Sci.*, 11 (2016) 2659.
14. H. Sepehri-Amin, T. Ohkubo, S. Nagashima, M. Yano, T. Shoji, A. Kato, T. Schrefl, K. Hono, *Acta Mater.*, 61 (2013) 6622.
15. H.X. Zeng, Z.W. Liu, W. Li, J.S. Zhang, L.Z. Zhao, X.C. Zhong, H.Y. Yu, *J. Magn. Magn. Mater.*, 471 (2019) 97.
16. Y.I. Lee, Y.J. Wong, H.W. Chang, W.C. Chang, *J. Magn. Magn. Mater.*, 478 (2019) 43.
17. J.T. Li, M.X. Pan, Y.D. Yu, H.L. Ge, Q. Wu, *Int. J. Electrochem. Sci.*, 13 (2018) 8897.
18. H. Kanekiyo, M. Uehara, S. Hirosawa, *Mater. Sci. Eng. A*, 181-182 (1994) 868.
19. J.J. Ni, T.Y. Ma, M. Yan, *Mater. Lett.*, 75 (2012) 1.
20. Y.R. Wu, J.J. Ni, T.Y. Ma, M. Yan, *Physica B*, 405 (2010) 3303.
21. P. Zhang, L.P. Liang, J.Y. Jin, Y.J. Zhang, X.L. Liu, M. Yan, *J. Alloys Compd.*, 616 (2014) 345